Available online at www.sciencedirect.com
ScienceDirect
Nuclear Science and Techniques 19 (2008) 178–186
NUCLEAR SCIENCE AND TECHNIQUES

Numerical analysis of thermal-hydraulic behavior of supercritical water in vertical upward/downward flow channels

GU Hanyang* YU Yiqi CHENG Xu LIU Xiaojing

School of Nuclear Science and Engineering, Shanghai Jiaotong University, Shanghai 200240, China

Abstract Investigations on the thermal-hydraulic behavior in the SCWR fuel assembly have obtained a significant attention in the international SCWR community. However, there is still a lack of understanding of the heat transfer behavior of supercritical fluids. In this paper, the numerical analysis is carried out to study the thermal-hydraulic behaviour in vertical sub-channels cooled by supercritical water. Remarkable differences in characteristics of secondary flow are found, especially in square lattice, between the upward flow and downward flow. The turbulence mixing across sub-channel gap for downward flow is much stronger than that for upward flow in wide lattice when the bulk temperature is lower than pseudo-critical point temperature. For downward flow, heat transfer deterioration phenomenon is suppressed with respect to the case of upward flow at the same conditions.

Key words Supercritical water reactor, CFD, Heat transfer

CLC number TL331

1 Introduction

Supercritical water-cooled reactor (SCWR) is characterized as low flow rate, high enthalpy rise, and single-phase water-cooling, with which high thermal efficiency is achieved. Design of SCWR is based on the proven LWR technology and experiences of fossil power plants with supercritical steam conditions. The role of SCWR has been emphasized on economical electricity generation for near- or mid-term nuclear market. The SCWR has been regarded as an innovative reactor and selected as one of candidates of Generation IV reactor systems. Research efforts have been made worldwide to develop SCWR type nuclear power plants[1-5].

A main feature of supercritical water is the strong variation of its thermal-physical properties in the vicinity of the pseudo-critical line. This leads to an unusual flow and heat transfer behavior. Therefore, a reliable knowledge of the thermal-hydraulic behavior in reactor relevant conditions is of great importance in designing a SCWR core. Studies on thermal-hydraulic behavior of supercritical fluids can be traced back to the 1950s. Experimental and theoretical studies on heat transfer in supercritical pressure conditions were reviewed in Refs. [6-10]. Pioro and Duffey [10] found that a majority of the experimental data were obtained in vertical tubes, while Silin *et al*. [11] performed an experiment on heat transfer in larger bundles at supercritical pressures and found that the heat transfer data could be satisfactorily described by correlations obtained for water flow in tubes at supercritical pressures for normal heat transfer regime, but no heat transfer deterioration (HTD) in rod bundles were observed within the same test parameter range for which heat transfer deterioration occurred in tubes. It is noticed that the experimental investigations devoted to heat transfer in bundles cooled with water at supercritical pressures are very limited, and more research efforts must be made to provide reliable information for SCWR designs.

Due to limited measurement techniques,

Supported by National Basic Research Program of China (No. 2007CB209804).

*Corresponding author. E-mail: guhanyang@stju.edu.cn

Received date: 2008-03-25

numerical investigations using Computational Fluid Dynamics (CFD) codes is great help for a better understanding of the heat transfer mechanism. But difficulties in the numerical analysis are related to the turbulence modeling at supercritical pressures. In the earlier works, turbulence modeling was based on simple eddy diffusivity approaches[12]. Qualitatively, the numerical prediction agrees with the experimental data. In spite of quantitative deviations between the numerical and experimental results, CFD is a suitable approach for analyzing the thermal-hydraulic behavior of supercritical fluids. In recent years, with increased computer capability, advanced turbulence models have been increasingly applied to numerical studies. Due to a sharp variation of properties near the heated wall, either a fine numerical mesh structure or a suitable wall treatment is necessary. During the past a few years, extensive efforts have been made to assess the applicability of existing CFD codes to the heat transfer simulation at supercritical pressures. In comparing their results of numerical analysis using over 10 first order closure turbulence models to experimental data for upward flows in circular tube, Kim *et al*. [13] found that RNG k–ε model with enhanced near-wall treatment gave the most outstanding prediction. This was confirmed by Roelof and Komen [14]. Yang *et al*.[15] used 13 turbulent models to study heat transfer in upward flows of supercritical water in circular tubes with different wall treatment in STAR-CD3.24, and found that both two-layer model [16] and standard k–ε high Re model with the standard wall function gave acceptable prediction. In flow channels other than a circular tube, e.g. the typical flow channels of a SCWR fuel assembly, anisotropic behavior of turbulence and secondary flow occurred [17-20]. Thus, turbulence models, which are capable of simulating anisotropic behavior of turbulence, are highly required for analyzing heat transfer in sub-channels. Using CFX5.6, Cheng *et al*. [21] studied the effect of mesh structures and turbulence models on heat transfer of supercritical water. Based on the circular tube studies, and due to capability requirement on simulating anisotropic behavior of turbulence, the SSG Reynolds stress model is recommended for sub-channel geometry applications.

Most of the numerical studies on heat transfer of supercritical fluids were done with simple flow channel geometries, e.g. circular tubes, but outcomes in circular tubes cannot be directly extrapolated to non-circular flow channel. Also, few studies have been done on thermal-hydraulic behavior for downward flow. To avoid overheated fuel pins in hot channel and to achieve higher core exit temperatures, Shulenberg *et al* [4] proposed several multi-flow pass SCWR core structure designs, in which both downward and upward flow existed in fuel assemblies. In this paper, numerical analysis is carried out to provide basic understanding of supercritical water thermal-hydraulic behavior in vertical upward/downward flow channels.

2 Computational procedures

In the present study, regular sub-channels of bare rod bundles are considered, both in square and in triangular arrangement (Fig.1). Due to the symmetric feature, only 1/4 of a regular sub-channel of the square lattice and 1/3 of a regular sub-channel of the triangular lattice are taken as computational domain for the CFD analysis, with the Reynolds number of 51,000 at the sub-channel inlet. The other parameters (Table 1) were decided according to those widely used in SCWRs[21]. The thermal physical properties of water were taken from Ref. [22]. In all simulations, a constant wall heat flux was added on the fuel wall, with application of the second order closure turbulence model SSG, which, among all the four ε-type models in CFX5.6, is the only turbulence model capable of simulating the anisotropic behavior of turbulence.

3 Results and discussion

3.1 Flow pattern

Fig.2 shows the projection of velocity vector on the X-Y plane in square and triangular lattices at various pitch-to-diameter ratios for upward and downward flows. The bulk fluid temperature on the elevation is 384^{o}C, very close to the pseudo-critical value. It can be seen that secondary flow appears in all rod bundles. One secondary flow cell can be found in each one-eighth sub-channel of the tight square lattice with P/D=1.2, while the direction of secondary flow is opposite in two conditions. Considering that the mean axial velocity is 2.3 m·s^{-1} in the square lattice with

P/*D*=1.2, the maximum velocity of the secondary flow in tight square lattice is about 0.36% and 0.44% of the mean axial velocity for upward and downward flow, respectively. There are two secondary flow cells in the wide square lattice with *P*/*D*=1.4 for upward flow, while only one cell is observed in the same condition for downward flow. The maximum velocity of the secondary flow in the wide triangular lattice of *P*/*D*=1.4 is about 0.22% and 0.18% of the mean axial velocity for upward and downward flow, respectively. These agree well with the experimental findings in Refs. [18,23,24].The secondary flow for upward flow is much stronger than that for downward flow in triangular lattice with *P*/*D*=1.4 at T_b=384°C (Fig.2c), as the secondary flow is in square lattice rather than in triangular lattice at same pitch-to-diameter ratio.

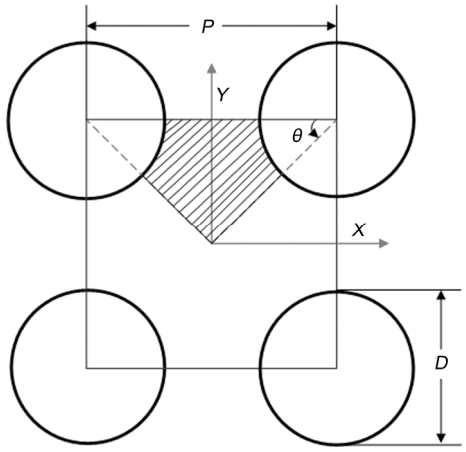

(a) Square lattice

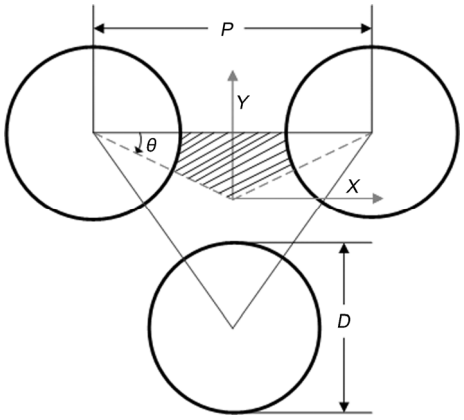

(b) Triangular lattice

Fig.1 Sub-channels configuration.

Table 1 Parameters used for the CFX simulation

Parameters	Range
Rod bundle arrangement	Square, triangular
Rod diameter / mm	8.0
Pitch-to-diameter ratio	1.1 – 1.4
Rod length / m	4 .0
Pressure / MPa	25.0
Mass flux / kg·m^{-2}s^{-1}	350– 2000
Wall heat flux / kW·m^{-2}	600
Fluid bulk temperature / °C	280– 510
Reynolds number	51,000 – 500,000
Turbulence model	SSG

To present the amplitude of secondary flow as a function of bulk temperature clearly, the parameter, dimensionless secondary flow energy, can be defined as

$$K = \frac{1}{A}\int_A mu_{sec}^2 \mathrm{d}A \Big/ \frac{1}{A}\int_A mw^2 \mathrm{d}A = \int_A m(u+v)^2 \mathrm{d}A \Big/ \int_A mw^2 \mathrm{d}A \quad (1)$$

where *u*, *v* and *w* is the velocity along *X*, *Y* and *Z* axis, respectively.

Fig. 3 shows the dimensionless secondary flow energy versus the bulk temperature in the square lattice of *P*/*D*=1.1 and 1.4, respectively. In the tight square lattice with *P*/*D*=1.1 (Fig. 3a), the secondary flow energy decreases with increasing bulk temperature at a bulk temperature lower than the pseudo-critical value. The minimum secondary flow energy is achieved when the fluid temperature approaches the pseudo-critical value. The secondary flow energy increases with the bulk temperature that exceeds the pseudo-critical value. In addition, higher secondary flow energy can be obtained for downward flow. For example, when the fluid bulk temperature is 384°C, the secondary flow energy for downward flow is almost seven times that for upward flow. In contrary to the result for the tight square lattice, the secondary flow energy increases at first and then decreases with increasing bulk temperature for the wide square lattice with the maximum value occurring at pseudo-critical temperature, except downward flow at bulk temperature far lower than pseudo-critical temperature. Except for the pseudo-critical region, the secondary flow energy for downward flow is higher than that for upward flow in wide square lattice.

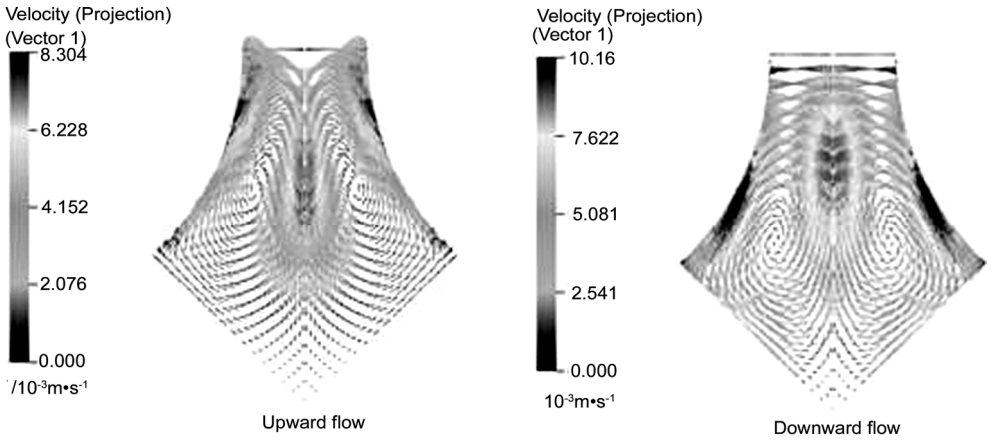

(a)*P*/*D*=1.2, square lattice

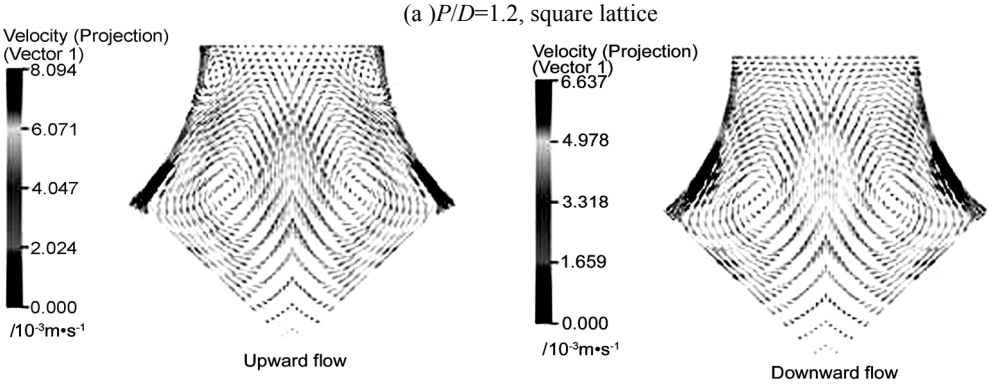

b)*P*/*D*=1.4, square lattice

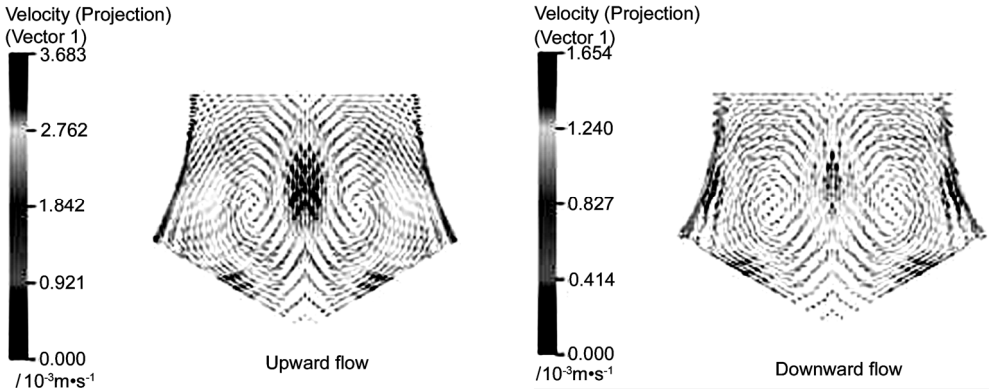

(c)*P*/*D*=1.4, triangular lattice

Fig.2 Flow patterns in square and triangular bundle lattices (T_b=384°C).

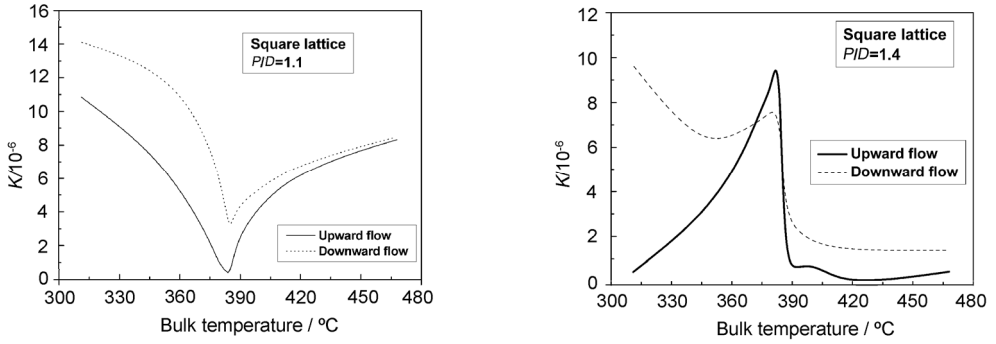

(a) *P*/*D*=1.1 (b) *P*/*D*=1.4

Fig.3 Secondary flow energy in square lattice at two *P*/*D* ratios.

The effect of pitch-to-diameter ratio on the secondary flow energy in a triangular lattice is similar to that in a square lattice for upward flow (Fig.4). But in contrary to the result for the tight square lattice, the secondary flow energy is stronger for upward flow than that for downward flow in tight triangular lattice, except in the vicinity of the pseudo-critical region. Meanwhile, the secondary flow energy is much lower in the triangular lattice than that in the square lattice.

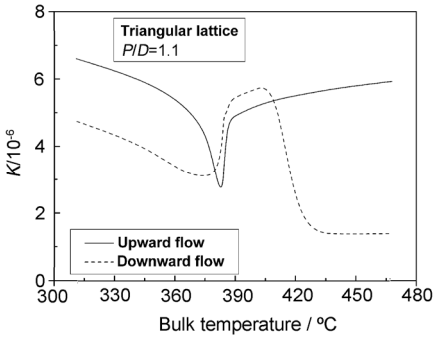

(a) P/D=1.1

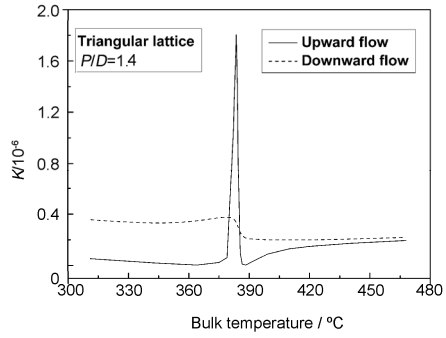

(b) P/D=1.4

Fig.4 Secondary flow energy in triangular lattice at two P/D ratios.

3.2 Turbulent mixing

From the definition of the Reynolds stress, which can be directly provided by the CFX calculation, one can obtain the relationship between the Reynolds stress $\overline{vv}$:

$$\overline{vv}=\frac{1}{T}\int_T v^2\mathrm{d}t \tag{2}$$

and the average amplitude of the velocity fluctuation across the gap $\overline{|v|}$:

$$\overline{|v|}=\frac{1}{T}\int_T |v|\cdot\mathrm{d}t \tag{3}$$

It yields

$$\overline{vv}=\frac{1}{T}\int_T v^2\mathrm{d}t=\frac{1}{T}\int_T\left(\overline{|v|}^2+v'^2\right)\mathrm{d}t$$
$$=\overline{|v|}^2+\frac{1}{T}\int_T v'^2\mathrm{d}t\geq\overline{|v|}^2 \tag{4}$$

In Eq. (4), T stands for the time interval considered, t for time, v for velocity fluctuation and v' for the deviation of the velocity fluctuation amplitude from the average value of the fluctuation amplitude, as defined below

$$v'=|v|-\overline{|v|}=|v|-\frac{1}{T}\int_0^T|v|\cdot\mathrm{d}t \tag{5}$$

The statistical feature of the velocity fluctuation in turbulent flows depends on flow conditions. However, according to some experimental information available, the Gaussian distribution of the probability distribution was found, in many cases, to be a fairly good approximation for the velocity fluctuation [25]. Therefore, in this study, a Gaussian distribution of the probability distribution for the velocity fluctuation is assumed, i.e.

$$f(v)=\frac{1}{\sqrt{2\pi}\sigma}\mathrm{e}^{-\frac{v^2}{2\sigma^2}} \tag{6}$$

Using the probability density function, it yields

$$\overline{vv}=\int_0^\infty v^2\cdot f(v)\mathrm{d}v=\frac{\sigma^2}{2} \tag{7}$$

and

$$\overline{|v|}=\int_0^\infty v\cdot f(v)\mathrm{d}v=\frac{\sigma}{\sqrt{2\pi}} \tag{8}$$

From Eqs. (7) and (8), it yields

$$\overline{|v|}=\frac{\sqrt{\overline{vv}}}{\sqrt{\pi}} \tag{9}$$

Eq. (9) is used in the present study to derive the average amplitude of the velocity fluctuation across the gap by knowing the Reynolds stress, which is obtained from the CFD analysis.

Fig.5 shows the average amplitude of the velocity fluctuation across the gap normalized by the shear velocity, i.e. $c=\overline{|v|}/u_\tau$ in the square lattice of

P/D=1.2 at two different thermal boundary conditions. The shear velocity u_τ is calculated by

$$u_\tau = \sqrt{\frac{\tau_w}{\rho}} = \sqrt{\frac{f}{8}}\, w \tag{10}$$

Here τ_w is wall shear stress, ρ density, w axial mean flow velocity and f friction factor, which can be calculated using the conventional Blasius correlation

$$f = \frac{0.3164}{Re^{0.25}} \tag{11}$$

It has to be pointed out that Eq.(11) is valid for $Re<10^5$. However, its application is extrapolated to the entire parameter range considered in the present paper. From the results in Fig.5, the average amplitude of the velocity fluctuation across the gap has its maximum close to the wall. It decreases with the increasing distance to the wall. It can be found that the effect of Reynolds number on normalized velocity fluctuation in the gap of tight lattices is negligibly small. The effect of flow direction on the velocity fluctuation across the gap in the tight lattice is not so apparent.

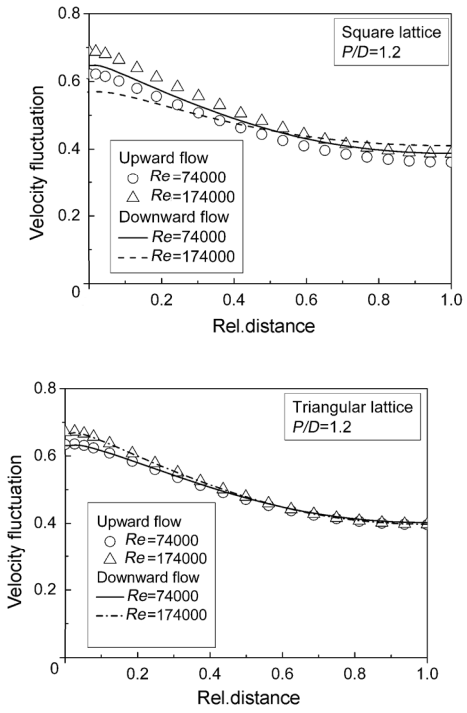

Fig.5 Effect of Reynolds number on normalized velocity fluctuation at the gap in square lattice.

According to the definition of turbulent mixing coefficient widely used in sub-channel analysis codes[26], the mixing coefficient can be derived as

$$\beta = \frac{|\overline{v}|}{W} = \frac{cu_\tau}{W} = 0.20cRe^{-0.125} \tag{12}$$

Eq. (12) has the similar form as that proposed by Rogers & Todreas. [27]

Fig. 6 shows the mixing coefficients across the gap versus bulk fluid temperature at various pitch-to-diameter ratios. Generally, CFD code gives similar behavior of mixing coefficients for both square and triangular arrangements. At a pitch-to-diameter ratio of < 1.3, the dependence of the mixing coefficient on the pitch-to-diameter ratio and bulk temperature is small, except that an abrupt fluctuation with small amplitude occurs in the vicinity of the pseudo-critical region. In the tight lattice, the effect of flow direction on turbulent mixing is small. In a wide lattice (P/D>1.3), the mixing coefficient decreases rapidly when bulk temperature approaches the pseudo-critical value for upward flow, while the sharp decrease in turbulent mixing coefficient is not seen for downward flow (Fig.6). So the turbulent mixing is much stronger for downward flow than that for upward flow in wide lattice with the bulk temperature lower than pseudo-critical point temperature. The mixing coefficient depends on sub-channel geometry as well as flow parameters as discussed in Ref. [28]. Further investi-gation with a wider range of parameters is needed.

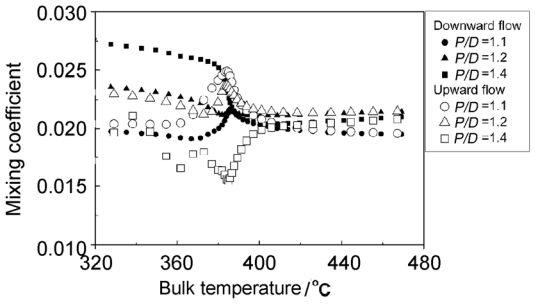

(a) Square lattice

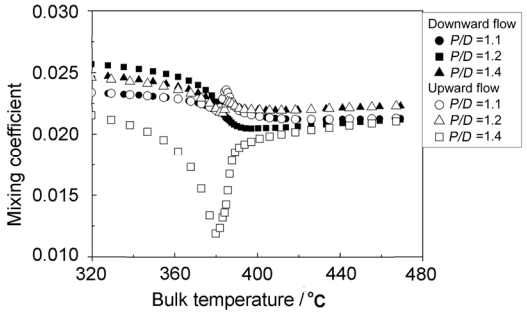

(b) Triangular lattice

Fig.6 Effect of pitch-to-diameter ratio on turbulent mixing coefficient.

3.3 Heat transfer

Local Nusselt number at different bulk fluid temperatures for upward and downward flow in square lattice with a pitch-to-diameter ratio of 1.2 is given in Fig.7, which shows the results on the rod surface along three lines, i.e. in the gap (θ=0°), on the symmetrical line (θ=45°), and on the center line (θ=22.5°). A circumferentially non-uniform distribution of the Nusselt number is clearly identified in both lattices. Generally, heat transfer in the gap (θ=0°) is less efficient. Heat transfer is enhanced by increasing the angle from the gap to the symmetric line. A much less non-uniformity in the circumferential distribution of Nusselt number can be seen in the vicinity of pseudo-critical temperature for downward flow compared with that for upward flow.

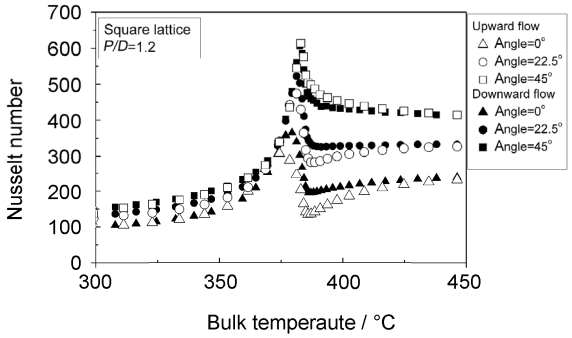

Fig.7 Nusselt number at various circumferential angles for square lattice.

Fig. 8 compares the calculated Nusselt number in both lattice arrangements with different pitch-to-diameter ratios for upward and downward flow. The results on the rod surface along the gap (θ=0°) is presented. In square lattice, at low bulk temperature, i.e. lower than pseudo-critical temperature, the flow direction has small effect on the transfer, owing to small buoyancy effect. In the vicinity of pseudo-critical temperature, the sharp change in density lead to significant buoyancy effect. A much stronger heat transfer is obtained for downward flow in this temperature region. Due to the higher fluid velocity in triangular lattice, a lower buoyancy effect is achieved, so the effect of flow direction on heat transfer in triangular lattice is not as strong as that do in square lattice except the wide lattice.

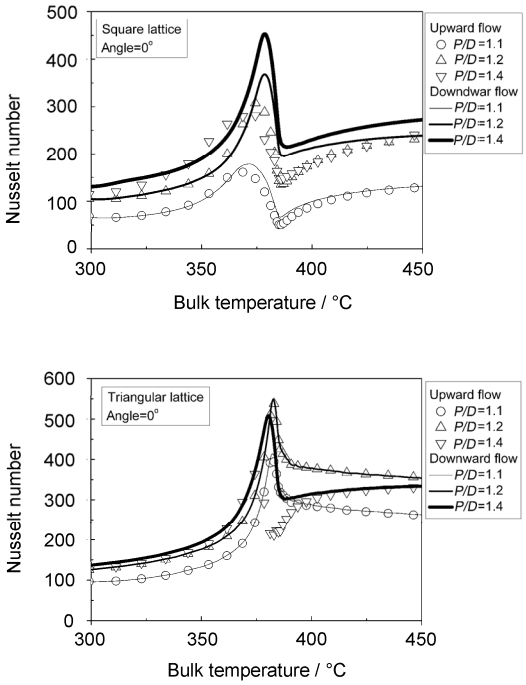

Fig.8 Nusselt number for square and triangular lattices at various circumferential angles and pitch-to-diameter ratios.

Fig.9 show velocity and turbulence energy distribution along the axial θ=22.5° on an elevation where the bulk fluid temperature is 384°C. For upward flow, both natural convection due to buoyancy effect and forced convection act in the same direction, the water is accelerated in the region close to the channel wall. Because of mass continuity, the flow is retarded in the core. Therefore, the velocity profile becomes steeper close to the walls and flattens in the center. The situation is vice versa for downward flow. The turbulence production depends on the difference between the velocity at the rim of the viscous layer and that in the core of the flow. So the turbulence production in downward flow is higher than that in upward flow as shown in Fig.9. According to Prandtl model[29], heat transfer to turbulent flows is controlled by two mechanisms in series, i.e. heat conduction through the viscous layer and diffusive energy transport from the border of viscous layer to the core of the turbulent flow, with the latter being the significant one. The diffusive energy transport is proportional to the turbulence production in the area close to the rim of the viscous layer. So the heat transfer is improved for downward flow.

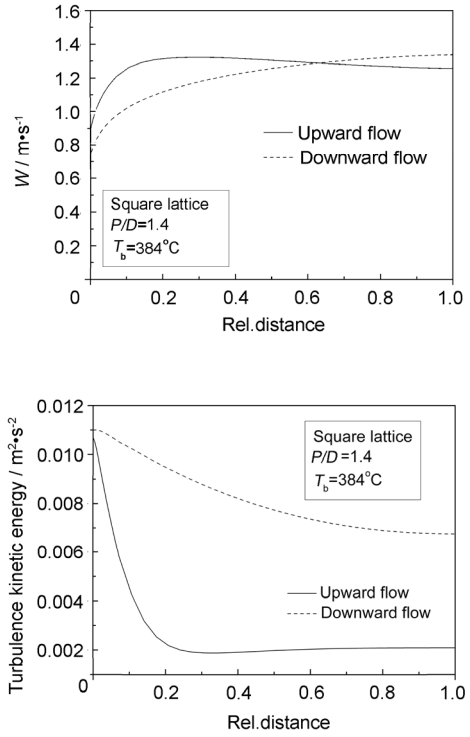

Fig.9 Velocity and turbulence energy distributions.

4 Summary

CFD analysis was carried out to gain basic knowledge of supercritical water flows in typical flow channels of SCWR fuel assemblies. The thermal-hydraulic behavior in the sub-channels of both upward and downward flow is analyzed. The results can be summarized as follows.

(1) The structure and amplitude of secondary flow cell mainly depends on geometric configuration of sub-channels as well as flow direction. The secondary flow energy in a square lattice is much larger than that in a triangular lattice at the same pitch-to-diameter ratio.

(2) The turbulent velocity fluctuation across the gap is an important parameter determining the inter-channel exchange. The results show that the velocity fluctuation is similar in both square and triangular lattices. It has the maximum value close to the wall surface and decreases with the distance to the wall. The effect of flow direction on velocity fluctuation is negligibly small in both lattice arrangements with small pitch-to-diameter ratios. While in wide lattice (P/D>1.3), the turbulent mixing for downward flow is much stronger than that for upward flow.

(3) A strong circumferential non-uniformity of wall temperature and heat transfer is observed in tight lattices, especially in square lattices for upward flow. The heat transfer is improved for downward flow compared with upward flow, especially in wide lattice.

Finally, it has to be pointed out that the conclusions achieved in this paper are only valid for the parameter ranges considered. Further analysis with a wider range of parameters is needed and underway.

References

1 Oka Y, Koshizuka S, Design concept of once-through cycle supercritical pressure light water cooled reactors. In: Proceeding of SCR. Tokyo, Japan, November 6-8, 2000, 1-22.

2 Yoo J, Ishiwatari Y, Oka Y, *et al*. Composite core design of high power density supercritical water cooled fast reactor. (Paper No.246) In: Proceeding of GLOBAL2005, Tsukuba, Japan, October 9-13,2005.

3 Kamei K, Yamaji A, Ishiwatari Y, *et al*. J Nucl Sci Technol, 2006, **43**:129-139.

4 Schulenberg T, Starflinger J, European research project on high performance light water reactors. In: Proceeding of SCWR-2007, Shanghai, China, March 12-15, 2007, 1-8.

5 Oka Y, Ishiwatari Y, Koshizuka S, Research and development of super LWR and super fast reactor. In: Proceeding of SCWR-2007, Shanghai, China, March.12-15, 2007, 9-18.

6 Jackson JD, Hall WB. Forced convection heat transfer to fluids at supercritical pressure. In: Kakaç S, Spalding D B (Eds.), Turbulent forced convection in channels and bundles, vol. 2. New York: Hemisphere Publishing Corp. 1979:563–612.

7 Polyakov A F, Adv. Heat Transfer, 1991, **21**:1-51.

8 Cheng X, Schulenberg T, Heat transfer at supercitical pressure-literature review and application to a HPLWR. Scientific Report FZKA6609.2001

9 Pioro I L, Khartabil H F, Duffey R.B. Nucl Eng Des ,2004, **230**: 69-91.

10 Pioro I L, Duffey RB. Nucl Eng Des, 2005, **235**:2407-2430.

11 [11]Silin V A, Voznesensky V A, Afrov A M. Nucl. Eng. Des,1993,**144**:327-336.

12 Shiralkar B S, Griffith P J. Heat Transfer,1969, **3**: 27-36

13 Kim S H, Kim Y I, Bae YY, *et al*. Numerical simulation of the vertical upward flow of water in a heated tube at supercritical pressure. Proc. ICAP,2004.

14 Roelof F, Komen Ed, CFD analysis of heat transfer to supercritical water flowing vertically upward in a tube, Jahrestagung Kerntechnik, Germany, 2005.

15 Yang J, Oka Y, Ishiwatari Y, *et al*. Nucl Eng Des.2007, **237**:420-430.

16 Hassid S, Poreh M, J Fluids Eng, 1978, **100**: 107-112.

17 Kjellström B, Studies of turbulent flow parallel to a rod bundle of triangular array. Report AE-RV-196, AB Atomenergi, Sweden,1971

18 Trupp A C, Azad R S. Nucl Eng Des, 1975, **32**: 47-84.

19 Vonka V. Nucl Eng Des, 1988, **106**:191-207.

20 Rehme K. Int J. Heat Mass Trans,1992,**18**: 1055-1069.

21 Cheng X, Kuang B, Yang Y H. Nucl Eng Des, 2007, **237:**240-252.

22 Wagner W, Kruse A. Properties of water and steam: The industrial standard IAPWS-IF97 for the thermodynamic properties and supplementary equations for other properties, Tables based on these equation, Berlin: Springer-Verlag, 1998.

23 Carajilescov P, Todreas N E. J Heat Transfer, 1976. **4**:262-268.

24 Cheng X, Tak N I. Nucl Eng Des. 2006, **236**: 1874-1885.

25 Lin C C, Statistical theory of turbulence. Princeton: Princeton University Press, 1961.

26 Stewart C W, COBRA-IV: The models and the methods. Battelle Pacific Northwest Laboratories, Report BNWL-2214, 1977.

27 Rogers J T, Todreas N E, Coolant inter-channel mixing in reactor fuel rod bundles single-phase coolant, in section heat transfer in rod bundle. In: The winter annual meeting of ASME, New York, 1968, 1-56.

28 Cheng X, Muller U. Int J Multiphase Flow, 1998, **24**:1245-1263.

29 Prandtl L, Führer durch die Strömungslehre, 3rd ed. Braunschweig: Vieweg, 1942.